HYDROTHERMAL SYNTHESIS (250°C) OF COPPER-SUBSTITUTED KAOLINITES

Sabine Petit,[1] Alain Decarreau,[1] Christine Mosser,[2]
Gabrielle Ehret,[3] and Olivier Grauby[4]

[1] "Argiles, Sols & Atérations", URA CNRS 721
Université de Poitiers, 40 Avenue du Recteur Pineau
F-86022 Poitiers Cedex, France

[2] Centre de Géochimie de la surface, UPR CNRS 6251
1 rue Blessig, 67084 Strasbourg Cedex, France

[3] IPCMS, CNRS, 23, rue du loess, F-67037 Strasbourg Cedex, France

[4] Centre de Recherche sur les Mécanismes de la Croissance Cristalline
UPR CNRS 7251, Campus de Luminy, Case 913, F-13288 Marseille, France

Abstract—To obtain Cu-kaolinites with a controlled range of chemical compositions, syntheses were performed by hydrothermally ageing gels with kaolinite stoichiometric compositions. Gels were prepared with sodium metasilicate and nitrates of octahedral cations. Temperature of synthesis was 250°C with a corresponding equilibrium water pressure of 38 bars.

Three samples with copper contents ranging from 0.1 to 7% and another one with the chemical composition of the Cu end-member were synthesized. While this fourth sample led to tenorite after the hydrothermal treatment, the three others crystallized well into kaolinite.

Up to almost 1% CuO was measured by TEM in some isolated 'clean' and hexagonal kaolinite particles. EPR and XPS spectroscopies were consistent with an octahedral position of Cu^{2+}. In IR spectra, νAl-OH-Cu absorption bands were not observed, but νAl$_2$OH bands appeared more and more blurred when Cu content of samples increased. Weak bands situated at 868 cm^{-1} and 840 cm^{-1} are tentatively attributed to δAlCuOH. By differential thermal analysis, a downward shift of 20°C in temperature of the endothermic peak from the less Cu-rich sample to the most Cu-rich one, argued for the existence of some Al-OH-Cu bonds, whose binding energies are presumed to be less than the Al-OH-Al ones.

In view of these results, Cu^{2+} appears incorporated in the octahedral sheet of kaolinite. Moreover, this incorporation is made without major perturbation of the kaolinite structure.

Key Words—Cu^{2+}, Kaolinite, Octahedral substitution, Synthesis.

INTRODUCTION

Unlike the other phyllosilicates, kaolinites show a nearly uniform chemistry, 46.5 wt. % SiO_2, 39.5 wt. % Al_2O_3, 14 wt. % H_2O, corresponding to the structural formula $Si_2Al_2O_5(OH)_4$. Typical chemical analyses show some variations in the major elements, but they are generally small. Small quantities of iron, titanium, potassium, and magnesium are also found. The presence of ancillary minerals in samples is to be expected, and sometimes these can be identified in X-ray diffraction patterns. The fact that deviations from the ideal stoichiometry are small suggests that ionic substitutions in the structure are few. Bulk chemical or other analytical methods are of little use because it is not possible to eliminate the contamination problem. Improvements in instrumentation, particularly in electron microscopy, both scanning and transmission, along with energy dispersive analysis have allowed the examination of individual particles of these minerals.

Very careful work, and the ability to "test" substitutions by the use of synthesis have shown that ferric iron can substitute for aluminium in octahedral sites (a review of this subject is made in Petit (1990)), even to a relatively high level in synthetic samples (Petit and Decarreau 1990), as well as gallium (Martin *et al* 1995). Chromium substitutions are evidenced in natural samples (Brookins 1973, Maksimovic and Brindley 1980, Maksimovic *et al* 1981, Shingh and Gilkes 1991, Mosser *et al* 1993). Ti is also considered as a potential candidate for substitution (Jepson and Rowse 1975, Rengasamy 1976, Weaver 1976).

Very few works deal with copper substitution in phyllosilicates, largely because Cu-rich clay minerals are not common in nature. The only well known Cu-rich phyllosilicate is chrysocolla which has an unclassical clay structure (Van Oosterwyck-Gastuche 1970). Medmontite, for example, initially described as a cupriferous saponite, was, in fact, characterized as being a mixture of chrysocolla and mica (Chukhrov *et al* 1969a 1969b). Natural examples of cupriferous clays show that copper is preferentially located in the interlayer space (Ildefonse *et al* 1986). In fact, the electronic properties of copper induce important distortions of octahedral sites due to the Jahn-Teller effect. This

Table 1. Expected (based on quantities used for synthesis) and measured by AAS, bulk chemical analyses (wt%) of starting materials; end of synthesis fluids chemical composition, and C.E.C. data of synthesized products.

Sample	Time (days)	Expected calculated values (%)				AAS measured values for gels (%)			Synthesis fluids (mg/l)			CEC (meq/100 g)
		c^*	SiO_2	Al_2O_3	CuO	SiO_2	Al_2O_3	CuO	Si	Al	Cu	
S1	21	0.003	54.0	45.9	0.1	52.3	47.6	0.1	/	/	/	6.5
S2	7	0.1	53.0	43.6	3.4	43.5	53.3	3.2	/	/	/	18.6
S3	7	0.2	51.9	41.2	6.9	47.8	47.5	4.7	152	6	0.7	16.0
S4	7	3.0	33.5	0	66.5	—	—	—	—	—	—	—

/: not measured because of solution leak during hydrothermal treatment.
*: c = amount of Cu according to the structural formula $Si_2Al_{2-2c/3}Cu_cO_5(OH)_4$.
—: not measured.

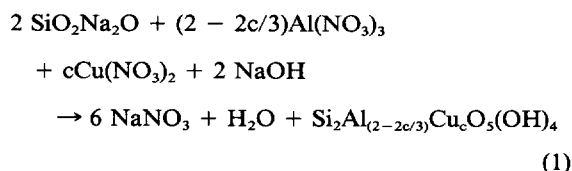property of Cu is not compatible with a regular clay structure (Wolff, 1967).

However, natural clay minerals with some Cu have been reported to occur, such as smectites with Cu content on the order of 2% (Mosser *et al* 1990, 1992). Previous experimental work showed that copper can be stabilized in a clay structure. For example, at high temperatures, cupriferous talcs and micas can be relatively easily synthesized (De Vynck 1980); Decarreau (1983) synthesized at 75°C (15 days) Cu-Mg smectites for Cu/Cu + Mg rates < 0.5. Chrysocolla was synthesized with higher Cu.

To determine limits of copper incorporation in kaolinites and to discuss more comprehensively its influence on clay structures, synthesis of Cu-substituted kaolinites at controlled Cu concentrations was attempted. Hydrothermal conditions (250°C) were chosen for synthesis in order to increase the rate of crystal growth. At ambient temperature, synthesis requires long ageing durations and produces poorly crystallized clays, whereas kaolinite is easily and rapidly obtained from hydrothermal experiments. A detailed review of this subject was given by Van Oosterwyck-Gastuche and La Iglesia (1978).

MATERIALS

Starting materials

Gels were prepared with sodium metasilicate (SiO_2 $Na_2O \cdot 5H_2O$) and aluminium and Cu(II) nitrates ($Al(NO_3)_3 \cdot 9H_2O$ and $Cu(NO_3)_2 \cdot 3H_2O$) according to the chemical reaction:

$$2\ SiO_2Na_2O + (2 - 2c/3)Al(NO_3)_3$$
$$+ cCu(NO_3)_2 + 2\ NaOH$$
$$\rightarrow 6\ NaNO_3 + H_2O + Si_2Al_{(2-2c/3)}Cu_cO_5(OH)_4$$
$$(1)$$

Four gels with different chemistries were prepared (Table 1). After precipitation, the solid phase was washed and centrifuged to remove sodium nitrate. Gels were then gently dehydrated at 70°C for 12 hours, then crushed. The initial products are X-ray amorphous,

except for the S4 sample (Table 1) which contains gerhardite (copper nitrate hydroxide).

Hydrothermal ageing

210 mg of powdered gels and 30 ml of distilled water were placed in Teflon-coated metallic bombs which were held at 250°C (±2°C), under the equilibrium water pressure (almost 38 bars). Synthesis time was seven days for samples S2, S3, and S4 and 21 days for S1 (Table 1).

Reference samples

The natural low-defect kaolinite GB3 which has been fully investigated by many authors (Cases *et al* 1982) was used as a reference. An amount of Cu <10 ppm was measured in this kaolinite (Liétard 1977).

METHODS

All samples were examined by X-ray diffraction (XRD) in reflection mode on powder preparations, using a Philips PW 1730 diffractometer equipped with Fe-filtered CoKα radiation (40 kV, 40 mA), combined with a DACO-MP computer. Because oriented preparations are difficult to obtain for synthetic samples, all the measurements were made from powder preparations.

The cation-exchange capacities (CEC) were measured by the ammonium-acetate method of Jackson (1958) at pH = 7.

Transmission electron microscopy (TEM) observations were made with a JEOL 2000 FX microscope using a beryllium grid holder and with samples dispersed on a carbon-coated Ni-microgrid. Chemical analyses were obtained by analytical electron microscopy (AEM), using the same microscope (200 kV accelerating voltage) equipped with energy dispersive X-ray analytical spectrometer (EDX, Tracor Northern Si(Li) detector). In fixed transmission mode, the spot size diameter ranged from 400 to 1000 Å. The thickness of the particles analysed being less than 1000 Å, quantitative data were obtained by the thin-film method (Cliff and Lorimer 1975) after calibration of the $k_{Al,Si}$ factors against natural and synthetic layer silicates

of known and homogeneous composition. The k_{Cu} factor was that of the manufacturer.

A NETZCH STA 409 EP with temperature programmer 410 and data acquisition system 414/0 controlled by computer was used for differential scanning calorimetry (DSC) and thermogravimetry (TG) thermal analyses. The curves were obtained with 20 mg samples heated at 10°C/mn in air.

Electron Paramagnetic Resonance (EPR) measurements were performed at 293°K on a X-band JEOL JEF-RE2X EPR spectrometer, equipped with a double cavity, using 100 kHz modulation and 20 mW incident microwave power. Calibrated quartz tubes of 4 mm internal diameter were filled to a depth of 3 mm with a weighed quantity of powdered air dried sample. A flat quartz cell covered with a removable quartz slide was used for wet samples soaked in water for more than 48 hours.

X-ray Photoelectron Spectroscopy (XPS) spectra were recorded on a CAMECA-RIBER NANOSCAN 50 apparatus equipped with an Al $K\alpha$ source and a MAC 2 analyzer which was set at 1 eV energy resolution. Samples were dispersed in distilled water by ultrasonic treatment. A drop of that dispersion was placed on a 2 cm disk of refractory vitreous carbon, air dried, and analyzed by XPS spectroscopy. Compensation for sample charging was made by setting the binding energies relative to the C ls line at 284.6 eV. This carbon was present due to hydrocarbon contamination.

Fourier Transform Infrared (FTIR) spectra were recorded in the 4800–200 cm^{-1} range on a Nicolet 510 FTIR spectrometer with a 4 cm^{-1} resolution. Spectra were obtained from KBr pressed pellets which were previously heated at 110°C overnight. These pellets were prepared by mixing a 2 mg sample with 300 mg KBr.

Chemical analyses of bulk samples were performed by atomic absorption spectroscopy (AAS) with a Perkin Elmer 2380 apparatus.

RESULTS

Chemical analyses

Owing to the small quantity of synthetic product obtained after synthesis (≈ 220 mg), AAS chemical analyses were only made on the starting gels. Because AAS chemical analyses on quenched synthesis fluids revealed cation concentrations in the ppm range (Table 1), bulk chemical compositions of the final synthesized products were assumed to be the same as those of the corresponding starting gels.

There is a discrepancy between the expected value and the measured one of chemical compositions (Table 1). The starting gels showed an excess in Al_2O_3 and a deficiency in SiO_2, significant for S2. It can be explained by the gel washing which preferentially carried away SiO_2. CuO measured values tend also to diminish
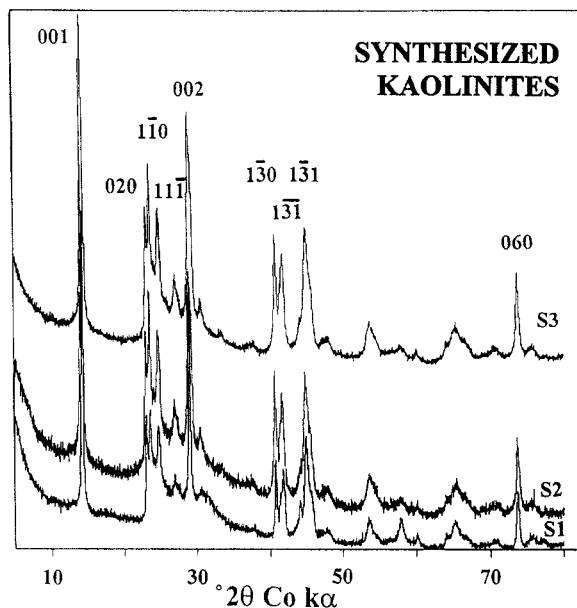

Figure 1.   XRD powder patterns of the synthesized products S1, S2, and S3.

relative to expected values with the increase of initial CuO introduced in the gels.

The CEC values of S1, S2, and S3 are respectively 6.5, 18.6, and 16 meq/100 g (Table 1).

XRD data

XRD spectra of all the studied samples are shown in Figure 1.

On the XRD patterns of S1, S2, and S3 samples, only reflections of kaolinite are observed (Brindley and Brown 1980), which is then the only one phase revealed. hkl reflections of kaolinite are narrow and well developed and no broad hump is present between 20 and 35° 2θ, indicating little or no amorphous residual product and good crystallization from the initial gels. For sample S4, tenorite (CuO) is the main component. Cuprite (Cu_2O) and small features corresponding to chrysocolla are also revealed in this sample. Because cupriferous clay minerals were not dominant components, no further studies were made on sample S4.

The 060 reflection is frequently used for the determination of the di- or trioctahedral nature of clays, a d(060) spacing of 1.48–1.50 Å characterizing a dioctahedral species and a spacing of 1.53–1.55 Å indicating a trioctahedral one (Brindley and Brown 1980). Detailed observations show that the 060 reflections are narrow and symmetrical for the 3 samples. The d(060) spacings of 1.49 Å clearly reveal the dioctahedral nature of these kaolinites, even for the most copper rich (S3) sample.

In contrast with the quantitative measure of disorder by computer fitting of XRD peak profiles (Plançon and
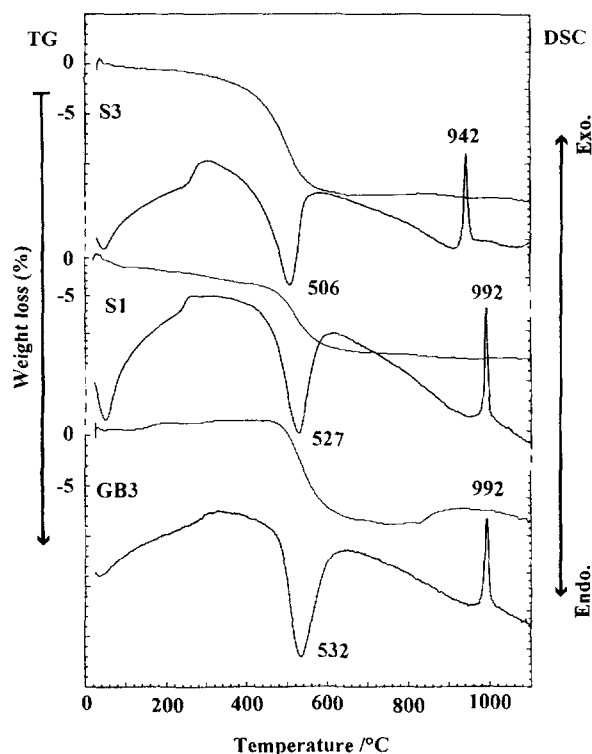
Figure 2.   TG and DSC curves of the S1 and S3 synthesized products and of the GB3 reference kaolinite.

Tchoubar 1977, Plançon *et al* 1989, Bookin *et al* 1989, Drits and Tchoubar 1990), Hi indices (according to Hinckley (1963)) are only semi-quantitative measures (Plançon *et al* 1988). Nevertheless, they are convenient to assign a numerical value to the degree of structural disorder (Brindley *et al* 1986). Kaolinites considered to be "well crystallized" give Hi > 1, whereas Hi ranges from 0.8 to 1 for kaolinites considered to be "medium crystallized", and Hi is lower than 0.8 for "poorly crystallized" kaolinites. For S1, S2, and S3 samples, the Hinckley indices are relatively high (respectively 0.92, 1.01, and 0.97) indicating a low level of structural defects.

For the 3 samples, the maxima of the $1\overline{3}1$ and $1\overline{3}1$ reflections are strongly drawn towards each other, indicating a marked monoclinic character (Plançon and Tchoubar 1977, Liétard 1977, Brindley and Porter 1978, Plançon *et al* 1989). Plançon *et al* (1989) showed by computer modelling that this monoclinic character is due to a high proportion of layers having vacant octahedral C sites (C layers), introduced as mistakes in the normal B-B-B. . .layer stacking sequence found in ordered kaolinites.

Thermal analyses

Thermal analyses were made on the reference GB3 and S1 and S3 kaolinites, but too little of S2 remained for analysis.

The DSC curves showed (Figure 2):

—a small low temperature endothermic peak at 45–50°C due to sorbed moisture;

—another small endothermic peak near 250°C, which is probably due to organic matter in the case of the reference, and dehydroxylation of not fully crystallized product in the case of S1 and S3 samples;

—the main relatively sharp dehydroxylation endothermic peak, located at 506°C, 526°C, and 532°C for, respectively, S1, S3, and the reference, corresponding to the transformation of kaolinite into metakaolinite;

—the characteristic sharp exothermic peak, corresponding to the spinel transition, occurring for S1 and the reference at 992°C, and for S3 at 942°C.

These data confirm the synthesis of the kaolinite polytype. Dickites give either broad peaks extending from about 500–700°C, or sharp peaks near 700°C (Brindley and Porter 1978).

The temperature of the main endothermic peak is known to be affected as much by particle size as by the mode of stacking of the layers (Mackenzie 1970, Liétard 1977, Cases *et al* 1982). In the case of synthesized kaolinites, De Kimpe *et al* (1981) and Petit (1990) observed, with increasing duration of hydrothermal treatment, an increase in the temperature of this endothermic peak, which they attributed to the improvement of sample crystallinity. On the other hand, the variability in temperature of the endothermic peak must in some way be connected with the energy of binding of the hydroxyl groups in the structure (Mackenzie 1970). Some contribution to peak temperature may be made by differences in chemical compositions as observed for minerals such as smectites and serpentines. For kaolinites, this factor has always been ignored since kaolinites are generally not appreciably substituted clays. In the present study, one must reconsider this in the light of the possibility of Cu^{2+} for Al^{3+} substitution.

The temperature and the broadness of the high temperature exothermic peak are only slightly linked with the characteristics of kaolinite itself, and are generally controlled by impurities closely associated with the kaolinite particles, detected by bulk chemical composition of samples (Liétard 1977). For S1 and S3, the sharpness of the peak probably indicates little or no 'impurities'; the almost 50°C difference between the peak position of the two samples is then more probably related to their respective copper contents.

The TG curves of the two Cu-substituted samples are very similar and differ from the reference kaolinite only by a more gradual continuous weight loss (Figure 2). The kaolinite/residual product ratio can then be either estimated (i) from the weight loss in TGA between 400°C and 650°C, as suggested by Tomura *et al* (1983), giving the proportion of strictly 'well crystallized' synthesized kaolinite or (ii) from the weight loss

between 250°C and 650°C, which corresponds to the dehydroxylation of all crystalline (more or less crystallized) forms of kaolinite. Using the second approach, 100% transformation of initial product into kaolinite was found for S1 and S3 samples which, as expected, is higher than that estimated by the first method (almost 75 and 80% for S1 and S3 respectively).

TEM data

1. Particle morphology. Various morphologies were observed:

—a classical pseudo-hexagonal platy morphology of kaolinite with typical electron diffraction pattern. The particle size is variable, but the majority of the particles are 0.3–0.5 μm long. They are often aggregated (Figure 3a). Some of them are rolled up (Figure 3b and 3c). This morphology prevails for S1, S2, and S3 samples.

— spherical particles (Figure 3b and 3c). They are numerous in S2 and S3 samples. Most of them lead to exfoliation (Figure 3b), and are clearly composed of numerous small irregular particles. Electron diffraction patterns are those of kaolinite giving either distinct halos or spots. At highest magnification and on the border of spherules, concentric stacking layers can be observed but they melt rapidly under the beam. Two main groups are observed: (i) with sizes of spherules ranging from 0.2 to 0.3 μm; (ii) with sizes less than 0.1 μm. Such spherules are often open (Figure 3c).

— very small amounts of residual, mostly non-reacted, product consisting of very fine particles, observed in the 3 synthetic samples. No particles with classical morphology of chrysocolla (i.e., fibers and colomnar particles (Van Oosterwyck-Gastuche 1970)) were observed.

2. AEM analyses. 35 chemical analyses (respectively 4, 20, and 11, for S1, S2, and S3, see Table 2) were carried out on (i) diffracting individual kaolinite particles, (ii) 'clean' aggregated crystals such as Figure 3a, (iii) spherical particles. No differentiation in chemical compositions can be made between these different morphologies.

The first main observation is, for the three samples, the inhomogeneity in the measured chemical compositions (Figure 4, Table 2):

— CuO contents show a large variability inside the expected range when a chemical solid-solution (expressed as oxides) is assumed between $Si_2Al_2O_7$ and $Si_2Al_{1.87}Cu_{0.2}O_7$ end-members;

— SiO_2 and Al_2O_3 measured contents are also variable, and are often outside the expected domain of chemical compositions calculated, for each sample, on a basis of a Cu-incorporation into kaolinite structure varying from 0 to c (see reaction (1) and Table 1).

Although some analyses show SiO_2 in excess, most of them show the reverse. Such observations about Si were made by both Calvert (1981) and Petit and De-

carreau (1990) for synthetic ferric kaolinites, and have also been noticed in the case of synthesis of pure Al-kaolinites (Fripiat and Gastuche 1961, Dennefeld 1970). Because no non crystalline Al phases was evidenced, these last authors concluded that Al may be incorporated more readily than Si into kaolinite.

From the CuO point of view, neither pure CuO nor Cu-rich product with an excess in SiO_2 relative to kaolinite were observed, indicating the absence of well crystallized copper oxide and 2:1 cupriferous clay particles. No major difference was seen between S2 and S3 samples, except that Cu-rich particles were relatively more numerous for S3. For the two samples, the measured CuO values were lower everywhere than might be expected (Table 2); that can not be verified for S1, whose low initial CuO content prevented AEM from measuring CuO amount within the accuracy limits of the method ($\approx$0–0.1%). Only two analyses gave CuO contents as high as $\approx$5% (Table 2), and in these two cases, the data must be questioned. The most Cu-rich analyzed particle did not diffract, but it may be amorphized under the beam. The other one was initially a relatively dark diffracting hexagonal kaolinite particle (Figure 3d); in this micrograph, the impact of the beam which causes amorphisation through the rounding off of borders of the particle can be observed. At the highest magnification, however some very small dark aggregates, which may have been Cu-rich contaminants, were revealed.

EPR measurements

EPR was used to identify the Cu^{2+} state (structural or exchangeable) in the samples. The position of Cu in exchangeable sites of kaolinites was studied with EPR spectroscopy by several authors (Sil'chenko *et al* 1971, McBride 1976, Pafomov *et al* 1979, Pilipenko *et al* 1987, 1989). McBride (1976) describes surface adsorbed Cu (II) on kaolinites as motionally restricted $Cu(H_2O)_4^{2+}$ when the kaolinite is air dried, and as rapidly tumbling $Cu(H_2O)_6^{2+}$ when water soaked. This causes a shift towards higher g values of the EPR signal when water soaked. Similar observations are well known for Cu-smectites (Clementz *et al* 1973, 1974; Mc Bride and Mortland 1974; Brown and Kevan 1988). Mosser *et al* (1990) showed that no shift was observed in the case of structural Cu in smectites. This observation was consistent with an octahedral position of Cu^{2+} where this element was trapped and could not tumble as it would in an interlamellar position.

EPR measurements were made on each sample in its air dried and wet states. The spectra show the characteristic Cu^{2+} signals (Figure 5), with distinct g// and g$\perp$ components. Since the g// values are higher than the g$\perp$ ones, the spectra are indicative of octahedral Cu^{2+} in an axially elongated tetragonal crystal field, with the unpaired electron occupying a $d(x^2 - y^2)$ orbital (Wertz and Bolton 1972).
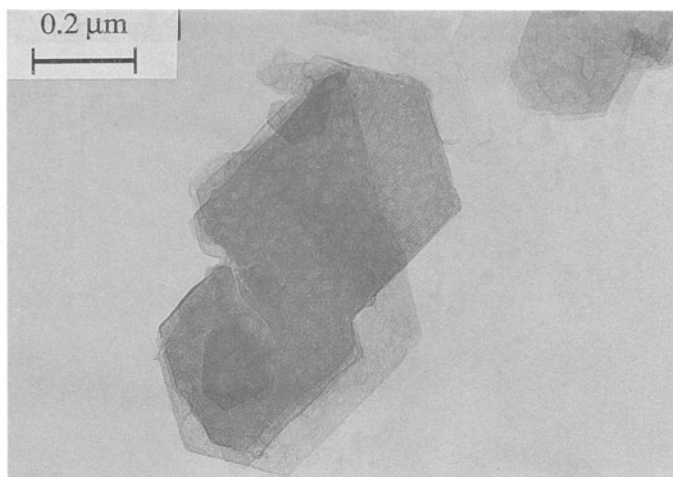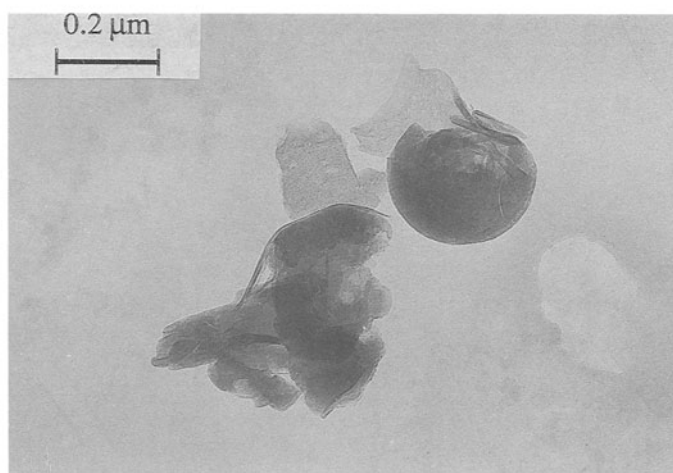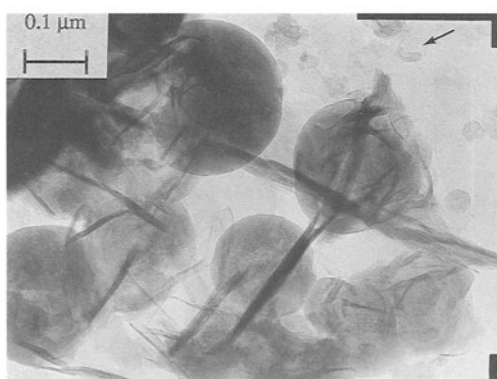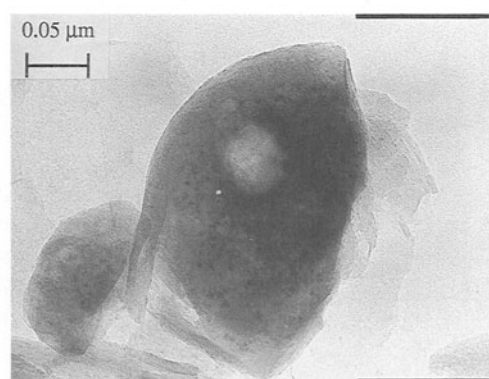
Figure 3. Electron micrographs of kaolinites synthesized at 250°C (7 days). A) platy particles (S2); B) spherical particles with exfoliation (S2); C) spherules and rolled up particles. The arrow shows an open little spherule (S3); D) impact of the beam and amorphization of an hexagonal particle (S3).

Table 2. Chemical composition of the synthetic samples S1, S2, and S3 obtained by TEM analyses of particles.

	SiO_2	Al_2O_3	CuO
S1	47.68	52.31	0.01
	56.15	43.84	0.01
	56.54	43.46	0.00
	49.38	50.61	0.01
S1 calc.*.**	54.0	45.9	0.1
S2	53.93	46.06	0.01
	53.09	46.57	0.34
	44.88	52.74	2.38
	52.70	46.25	1.05
	55.49	44.50	0.01
	54.15	45.82	0.03
	51.08	47.31	1.61
	57.42	42.50	0.08
	42.54	54.20	3.26
	40.00	54.06	5.94
	44.17	51.85	3.98
	56.32	43.66	0.02
	51.02	48.65	0.33
	56.32	43.67	0.01
	55.56	44.43	0.01
	44.41	55.35	0.24
	52.42	47.52	0.06
	51.95	48.01	0.04
	48.83	50.90	0.27
	45.83	54.06	0.11
S2 calc.*	53.0	43.6	3.4
S2 calc.**	53.3	43.1	3.6
S3	52.76	46.74	0.50
	57.54	42.08	0.38
	49.87	47.43	2.40
	52.00	47.51	0.49
	59.41	40.57	0.02
	47.10	47.60	5.30
	50.61	48.76	0.63
	48.41	49.27	2.32
	48.77	50.04	1.19
	44.79	51.85	3.36
	49.66	47.95	2.39
S3 calc.*	51.9	41.2	6.9
S3 calc.**	52.6	40.3	7.1

calc.: expected chemical compositions calculated.

* When supposing a mixed di-trioctahedral structure Si_2-$Al_{2-2c/3}Cu_cO_7$.

** When supposing a strictly dioctahedral structure Si_2-$Al_{2-c}Cu_cO_{7-c/2}$.

For the S1 and S2 samples, there is no upward shift of the $g\perp$ values when the air-dried kaolinites are water soaked (Figure 5). In fact, the $g\perp$ values of the water soaked samples are even slightly smaller than those of the air-dried samples, as previously observed by Mosser *et al* (1990) for synthetic smectites with structural Cu.

XPS data

In previous work (Mosser *et al* 1992), XPS was used to characterize the bonding state of Cu^{2+} in several phyllosilicates, including smectites, natural and synthetic (S3) kaolinites, and chrysocolla. From the comparison of the XPS spectra of these clays with those of
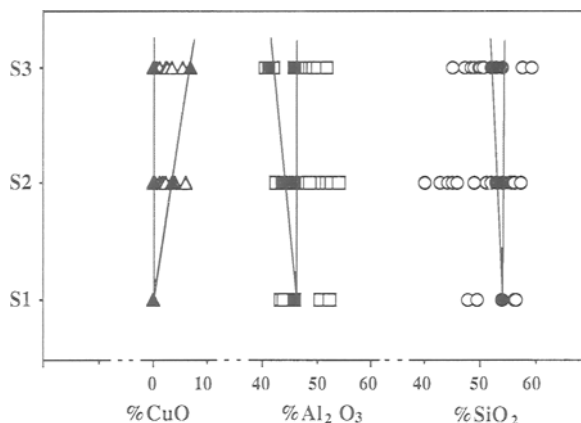

Figure 4. TEM chemical analyses data for S1, S2, and S3. Open symbols are measured data; solid symbols are calculated data. The greyish domain (delimited by calculated data) represents the extent of chemical variability related to a copper incorporation in the kaolinite structure varying, for each experiment, from 0 to c (according to an expected kaolinite structural formula: $Si_2Al_{(2-2c/3)}Cu_cO_5(OH)_4$); $\triangle$ CuO; $\square$ Al_2O_3; $\bigcirc$ SiO_2.

oxides with Cu in monovalent and divalent states, and after the study of photoreduction kinetics, the authors concluded that the S3 sample belongs to the group of clays with Cu^{2+} in octahedral sites.

FTIR data

The infrared spectra of samples S1, S2, and S3 are shown in Figures 6 and 7. The spectrum of the GB3 reference sample is also given for comparison.

1. OH stretching zone (Figure 6). The reference sample GB3 shows the 4 well resolved OH stretching bands, attributed to νAl_2OH group vibrations. The bands at 3695 and 3668 cm^{-1} are respectively in-phase and out-of-phase combination bands (Farmer 1964, 1974). The 3620 cm^{-1} band is undoubtedly attributed to the inner hydroxyl vibrations. However, the assignment of the 3652 cm^{-1} band is still controversial (Brindley *et al* 1986, Johnston *et al* 1990).

S1 differs from the GB3 reference sample only by the respective intensities of the 3668 and 3652 cm^{-1} bands, the latter one being more intense for the synthetic sample. This feature is frequently attributed to "poor crystallinity" of samples (Barrios *et al* 1977, Cases *et al* 1982) and more precisely, is empirically linked to monoclinic character of samples (Mestdagh *et al* 1982). The 4 Al_2OH bands are more and more blurred and broadened with increasing Cu-content of the samples, giving for S3, a broad band overlapping the well defined bands, with a clear feature at 3695 cm^{-1}.

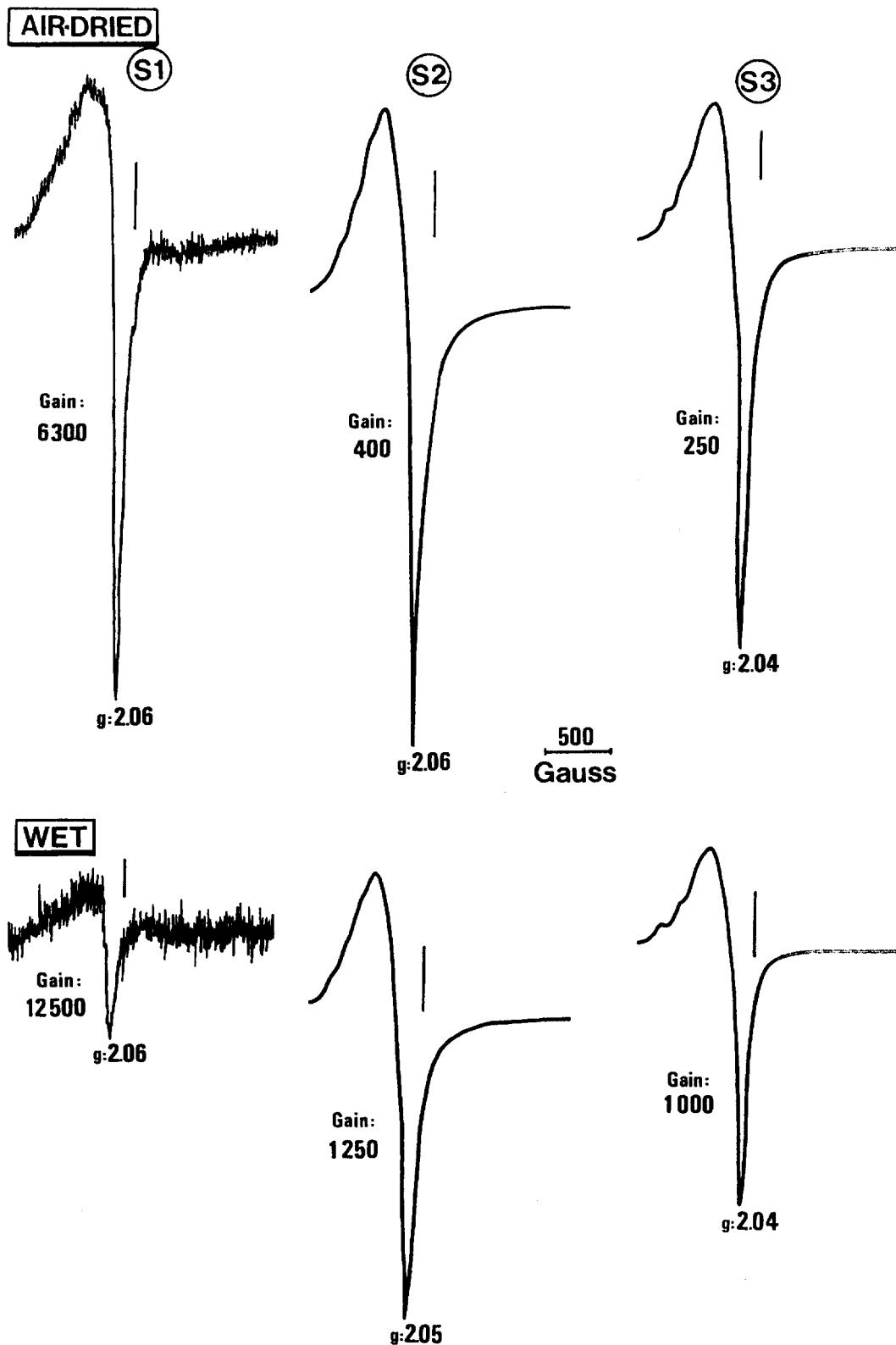No additional new band outside the Al_2OH group vibrations region can be observed.

Figure 5. EPR spectra of the synthesized products. The vertical lines represent the resonant position (g = 2.0028) of a standard strong pitch sample.
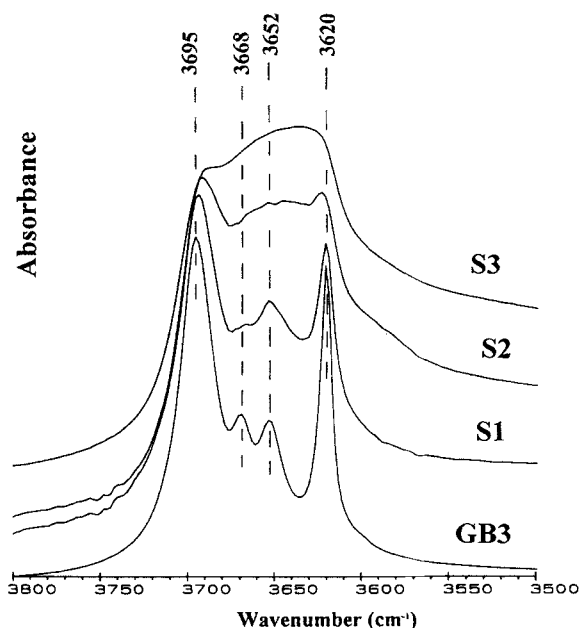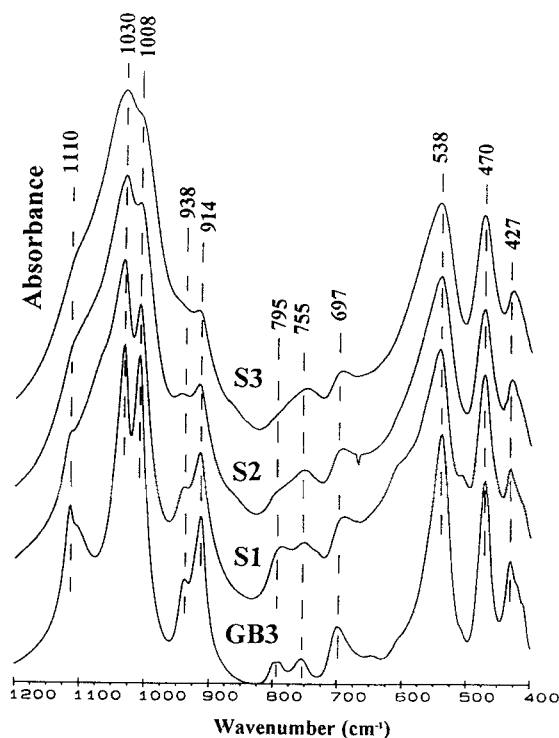
Figure 6. FTIR spectra in the OH stretching vibrations zone of the synthesized products S1, S2, S3, and the GB3 reference kaolinite.

2. The 1200–300 cm^{-1} region (Figure 7a). Spectra of all the samples show absorption bands for v and δ Si-O (respectively 1000–1100 cm^{-1}, 400–500 cm^{-1}), δ Al$_2$OH (914 cm^{-1} and shoulder at 938 cm^{-1}) and Al^{VI}-O-Si (538 cm^{-1}) and are very similar. However, with increasing Cu-content of the samples, a broadening of all the absorption bands is observed. The intensity of the δ Al$_2$OH vibration bands decreases with the Cu content of samples (see the expanded region (Figure 7B)). At the same time, for S2 and S3, a small shoulder centered near 868 cm^{-1} appears and tends to increase. Another band located at 840 cm^{-1} is also observed for S3. They are tentatively attributed to vibrations of the Al-OH-Cu group, because δ Al-OH-M (M = transitional metals like Fe^{3+}, or divalent cations such as Mg^{2+}, are classically observed in this region of IR spectra (Farmer 1974, Petit and Decarreau 1990, Grauby *et al* 1993).

DISCUSSION

Influence of copper on the experimental system

The synthesis of kaolinites is possible in copper-rich media (Cu contents ranged from 0 to almost 5% CuO). For synthesis without Al, in an attempt to obtain the hypothetical Cu end-member, the major synthesized component was tenorite and the only evidence of clay minerals was the possible occurrence of chrysocolla.
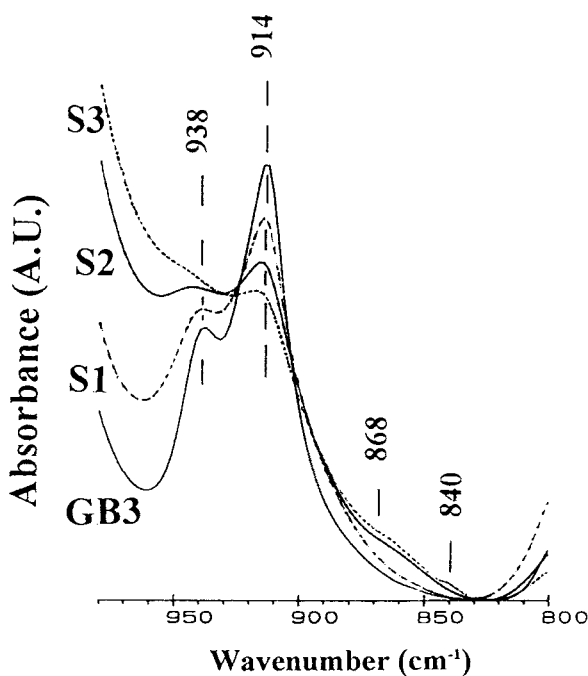

Figure 7. FTIR spectra of the synthesized products S1, S2, S3, and the GB3 reference kaolinite: a) in the 1200-400cm^{-1} region; b) details of the OH bending vibrations zone, normalized from the main Si-O vibrations band.

Further studies are necessary to determine at what Cu content the synthesis of kaolinite failed. When carrying out syntheses from amorphous starting materials and salt solutions of various concentrations, Miyawaki *et al* (1991) noted the inhibitory effect of divalent cations on the formation of kaolinite. They did not use Cu^{2+}, but they observed that kaolinite yields (measured from TG curves) and crystallinities were smaller when Ca^{2+} and Mg^{2+} rather than univalent cations such as Li^+, Na^+ or K^+ were introduced into the synthesis medium. This is not the case for Cu^{2+}, at least for the Cu-concentrations used here because: (i) Hinckley indices are indeed similar over the range of Cu content studied; (ii) % of transformation of initial products into kaolinite is even slightly higher when the Cu-concentration in the experimental system increases. Divalent transitional metals, like Cu^{2+}, do not act as poison in crystal growth of kaolinite.

Characterization of the synthesized samples

Kaolinite is the only crystallized product found in the studied S1, S2, and S3 samples.

Several morphologies including hexagonal and spherulitic, each of which can be possibly attributed to different types of kaolinite, are observed by TEM. Tomura *et al* (1983) described spherical morphology for synthetic kaolinites with only Si and Al as structural cations. They synthesized spherical kaolinites from amorphous material in hydrothermal experiments conducted between 150° and 250°C and under autogenous vapor pressure. Spherules formed around the starting material at 150° and 200°C, and platy or lath shaped kaolinites grew at the expense of the spherules at 250°C. Their TEM lattice images appeared to be concentric, but closer investigation showed that the spherical morphology was due to radiating columnar growth of kaolinite crystals and not to concentric layering of curved platy crystals as observed on halloysite spheres (Tomura *et al* 1985a). Tomura *et al* (1985b) concluded that the change of the morphology from spherical to platy with an increase in the reaction time indicates that the spherical form is metastable. It possibly explains the exfoliation observed in our micrographs and the scarcity of spherulitic particles in S1, which had a synthesis time greater than the two other samples (Table 1). Any copper influence on such morphology cannot be established from this study.

IR and XRD data revealed a strong monoclinic tendency for the kaolinites synthesized in media containing copper. It must be stressed that all kaolinites synthesized *at 250°C*, purely aluminous as well as iron-bearing ones, show such characteristics independent of the nature of substituted cations (Petit, 1990). This fact was less evident at lower temperatures (150°–200°C). No copper influence on monoclinic tendency could be established.

Further studies, such as XRD pattern decomposition, are required to characterize the different kaolinite phases (types and number of defects, etc.) revealed in synthetic Cu-bearing samples.

Copper location

EPR and XPS data are characteristic of Cu^{2+} in sites similar to those of octahedral sheets of phyllosilicates. So the occurrence of adsorbed or exchangeable Cu in synthesized kaolinites is completely excluded. However, Cu behavior in both starting gels and synthesized products is similar, using these two spectroscopic methods. EPR (and XPS) spectra of synthetic kaolinites can be then contaminated by the contribution of a residual product. However, XRD and TG data do not reveal, in the range of their detection limits, the occurrence of non crystalline, initial or residual, product. On the basis of these results, XPS and EPR signals can be attributed, for their majority, to Cu^{2+} cations in the octahedral sheet of kaolinite.

Because they are sensitive to cationic arrangement via hydroxyl bonds, other methods such as IR spectroscopy or thermal analyses should be more powerful to characterize Cu/Al substitutions in the octahedral sites of crystallized products like kaolinite, detecting Al-OH-Cu groups.

As seen above, the temperature of the endothermic peak is influenced by the particle size, % crystallization (=% transformation of initial gel into kaolinite) and chemical composition of samples. Because, (i) TG weight loss comparisons between S1, which is Cu-poor, and S3, which is more Cu-rich, are very close; and (ii) particles sizes are similar for all synthetic samples; then a difference of 20°C in temperature of the endothermic peak of these two S1 and S3 samples argues for the existence of Al-OH-Cu bonds.

In the literature, IR data for octahedral Cu in clays are found only for chrysocolla or trioctahedral talcs or micas (Wilkins and Ito 1967, De Vynck 1980). For chrysocolla, vCu_x-OH vibration bands are sharp and reported at 3650–3420 cm^{-1} (Chukhrov *et al* 1969b, Decarreau *et al* 1992), while the δCu_x-OH vibration band is located near 670 cm^{-1} (Sun 1963). For the spectra of synthesized products, such bands are unlikely to be observed because they are expected to occur only in the case of neighbouring Cu-Cu in the kaolinite octahedral sheet.

It has been observed that the intensity of the vAl_2OH and δAl_2OH bands decreases with the Cu content of samples. This is a strong argument for the occurrence of increasing Al/Cu substitutions in the octahedral sheet of synthetic kaolinites. Petit and Decarreau (1990) indeed observed in the case of synthetic ferric kaolinites that the decrease of the intensity of the Al_2OH vibration band does coincide with the increase of the structural iron content of kaolinites. Moreover, Stubican and Roy (1961) showed that there are more radical

changes when the substitution of ions with different charge takes place. For dioctahedral 2:1 clay minerals, the δAl_2OH vibration band decreases in intensity and is more poorly resolved with increasing amount of magnesium in the octahedral sheet.

On the other hand, weak bands situated at 868 cm^{-1} and 840 cm^{-1} are tentatively attributed to $\delta AlCuOH$.

Quantification of structural Cu

A high variability was observed in SiO_2 and Al_2O_3 values measured by AEM in synthesized kaolinite particles. The variability was equivalent for the three synthetic kaolinites (even for S1 sample which contains small amounts of CuO (0 to 1%)), and so cannot be related to Cu occurrence in the synthesis environment.

Due to the SiO_2 depletion observed in AEM chemical analyses of kaolinite particles, structural formulae have not been calculated. Though the highest CuO contents measured by AEM (5% and above) can be interpreted as contamination by condensed Cu-phases, the substitution of Cu for Al in kaolinite can easily reach amounts as high as the percent range.

On the other hand, clay particles from a same sample (S1, S2, or S3) exhibit chemical compositions which are more or less dispersed, as it has already been observed for other clay samples, synthetic ones, like Fe-kaolinites (Petit and Decarreau 1990), Al-Mg and Fe-Mg smectites (Grauby *et al* 1993, 1994), as well as natural ones (e.g., Paquet *et al* 1982, Petit *et al* 1992). In the case of synthetic samples, for which chemical variability cannot be explained by local variations in fluids chemical composition (they are not completely excluded, but they are unlikely to occur), this gives strong evidence for out of equilibrium crystallization of these clays.

Modality of the Al/Cu substitution

It is difficult to know whether the substitution obeys overall structural charge balance ($3Cu^{2+}$ for $2Al^{3+}$ substitution). This situation does not occur probably because features corresponding to Cu^{2+} neighbouring in octahedral sheet of kaolinites were not observed on IR spectra, even for the more Cu-rich kaolinite. However, CEC data argue for the possibility of some $1Cu^{2+}$ for $1Al^{3+}$ substitutions with a charge imbalance. XRD gives d(060) spacings of 1.49 Å, supporting the dioctahedral nature of Cu-substituted kaolinites.

CONCLUSION

For a long time, kaolinite was considered to have no substitution. In fact, various analytical techniques show the possibility of octahedral substitutions in some extent, for this mineral. It can be considered that at least about one percent for Cr^{3+} (Mosser *et al* 1993), and more for Fe^{3+} (Petit and Decarreau 1990) and Ga^{3+}

(Martin *et al* 1995) can be incorporated into the kaolinite structure.

There is strong evidence from this study, that a divalent cation such as Cu^{2+} substitutes for Al^{3+} in the kaolinite octahedral sheet. This substitution, which occurs at relatively low level (in the percent range), is made without major perturbations of the kaolinite structure. The dioctahedral nature of kaolinites appears to be wholly preserved, explaining the small incorporation of Cu in this mineral.

REFERENCES

Barrios J., A. Plançon M. I. Cruz, and C. Tchoubar. 1977. Qualitative and quantitative study of stacking faults in a hydrazine treated kaolinite—Relationship with infrared spectra. *Clays Clay Miner.* **25**: 422–429.

Bookin, A. S., V. A. Drits, A. Plançon, and C. Tchoubar. 1989. Stacking faults in kaolin-group minerals in the light of real structural features. *Clays Clay Miner.* **37**: 297–307.

Brindley, G. W., and A. R. D. Porter. 1978. Occurrence of dickite in Jamaica—Ordered and disordered varieties. *Amer. Miner.* **63**: 554–562.

Brindley, G. W., and G. Brown. 1980. *Crystal Structures of Clay Minerals and their X-Ray Identification.* London: Mineralogical Society, 495 pp.

Brindley, G. W., C. C. Kao, J. L. Harrison, M. Lipsicas, and R. Raythatha. 1986. Relation between structural disorder and other characteristics of kaolinites and dickites. *Clays Clay Miner.* **34**: 239–249.

Brookins, D. G. 1973. Chemical and X-ray investigation of chromiferous kaolinite ("miloschite") from The Geysers, Sonoma County, California. *Clays Clay Miner.* **21**: 421–422.

Brown, D. R., and L. Kevan. 1988. Aqueous coordination and location of exchangeable Cu^{2+} cations in montmorillonite clay studied by electron spin resonance and electron spin-echo modulation. *J. Amer. Soc.* **110**: 2743–2748.

Calvert, C. S. 1981. *Chemistry and Mineralogy of Iron Substituted Kaolinite in Natural and Synthetic Systems.* Ann Arbor, Michigan: University Microfilms International, 224 pp.

Cases, J. M., O. Liétard, J. Yvon, and J. F. Delon. 1982. Etude des propriétés cristallochimiques, morphologiques, superficielles de kaolinites désordonnées. *Bull. Mineral.* **105**: 439–455.

Chukhrov, F. V., B. B. Zvyagin, A. I. Gorshikov, L. P. Yermilova, and Y. S. Rudniskaya. 1969a. The nature of medmontite. *Int. Geol. Rev.* **11**: 1355–1359.

Chukhrov F. V., B. B. Zvyagin, L. P. Yermilova, A. I. Gorshikov, and Y. S. Rudniskaya. 1969b. *The Relation Between Chrysocolla, Medmontite and Copper-Halloysite.* Proc. Int. Clay Conf., Tokyo, 141–150.

Clementz, D. M., T. J. Pinnavaia, and M. M. Mortland. 1973. Stereochemistry of hydrated copper (II) ions on the interlamellar surfaces of layer silicates. An electron spin resonance study. *J. Phys. Chem.* **77**: 196–200.

Clementz, D. M., M. M. Mortland, and T. J. Pinnavaia. 1974. Properties of reduced charge montmorillonites: Hydrated Cu(II) ions as a spectroscopic probe. *Clays Clay Miner.* **22**: 49–57.

Cliff, G., and G. W. Lorimer. 1975. The quantitative analysis of thin specimens. *J. Microscopy* **103**: 203–207.

Decarreau, A. 1983. Etude expérimentale de la cristallogenèse des smectites. Mesure des coefficients de partage smectite trioctaédrique-solution acqueuse pour les métaux M²⁺ de la première série de transition. *Mém. Sci. Géol.* **74**: 190 pp.

Decarreau A., O. Grauby, and S. Petit. 1992. The actual distribution of octahedral cations in 2:1 clay minerals: results from clay synthesis. *Applied Clay Science* 7: 147–167.

De Kimpe, C. R., H. Kodama, and R. Rivard. 1981. Hydrothermal formation of a kaolinite-like product from noncrystalline aluminosilicate gels. *Clays Clay Miner.* **29**: 446–450.

Dennefeld, F. 1970. Contribution à la synthèse des phyllites alumineuses du type kaolin. Thesis, Univ. Strasbourg, France.

De Vynck, I. 1980. Synthèse de phyllosilicates de cobalt, de nickel, de cuivre et de zinc. *Silicates Industriels* **3**: 51–66.

Drits, V. A., and C. Tchoubar. 1990. *X-ray Diffraction by Disordered Lamellar Structures. Theory and Applications to Microdivided Silicates and Carbons.* Berlin Heidelberg: Springer Verlag. 371 pp.

Fartner, V. C. 1964. Infrared absorption of hydroxyl groups in kaolinite. *Science,* **145**: 1189–1190.

Farmer, V. C. 1974. The layer silicates. In *The Infrared Spectra of Minerals.* V. C. Farmer, ed. London: Mineralogical Society, 331–365.

Fripiat, J. J., and M. C. Gastuche. 1961. *Réflexions sur les problèmes de synthèse.* Coll. Int. CNRS, n°105, Genèse et synthèse des Argiles, Paris, 207–210.

Grauby, O., S. Petit, A. Decarreau, and A. Baronnet. 1993. The beidellite-saponite series: An experimental approach. *Eur. J. Mineral.* **5**: 623–635.

Grauby, O., S. Petit, A. Decarreau, and A. Baronnet. 1993. The nontronite-saponite series: An experimental approach. *Eur. J. Mineral.* **6**: 99–112.

Hinckley, D. N. 1963. Variability in "cristallinity" values among the kaolin deposits of the coastal plain of Georgia and South Carolina. *Clays Clay Miner.* **13**: 229–235.

Ildefonse, P., A. Manceau, D. Prost, and M. C. Toledo-Groke. 1986. Hydroxy-Cu vermiculite formed by the weathering of Fe-biotites at Salobo, Carajas, Brazil. *Clays Clay Miner.* **34**: 338–345.

Jackson, M. L. 1958. *Soil Chemical Analysis.* 3rd ed. Englwoods Cliffs, New Jersey: Prentice Hall, 498 pp.

Jepson, W. B., and J. B. Rowse. 1975. The composition of kaolinite. An electron microscope microprobe study. *Clays Clay Miner.* **23**: 310–317.

Johnston, C. T., S. F. Agnew, and D. L. Bish. 1990. Polarized single-crystal Fourier-transform infrared microscopy of Ouray dickite and Keokuk kaolinite. *Clays Clay Miner.* **38**: 573–583.

Liétard, O. 1977. Contribution à l'étude des propriétés physicochimiques, cristallochimiques et morphologiques des kaolins. Thesis, Nancy, 320 pp.

Mackenzie, R. C. 1970. *Differential Thermal Analysis. Volume I: Fundamental Aspects.* A. C. Mackenzie, ed. London: Acad. Press, 775 pp.

Macksimovic, Z. and G. W. Brindley. 1980. Hydrothermal alteration of a serpentinite near Takovo, Yugoslavia, to chromium-bearing illite/smectite, kaolinite, tosudite, and halloysite. *Clays Clay Miner.* **28**: 295–302.

Macksimovic, Z., J. L. White, and M. Logar. 1981. Chromium-bearing kaolinite from Teslic, Yugoslavia. *Clays Clay Miner.* **29**: 213–218.

Martin, F., S. Petit, O. Grauby, Y. Noack, and A. Decarreau. 1995. Ga/Al substitutions in synthetic kaolinites and smectites: XRD, FTIR and TEM studies. *Clay Miner.* (in press).

McBride. 1976. Origin and position of exchange sites in kaolinite: An ESR study. *Clays Clay Miner.* **24**: 88–92.

McBride, M. B., and M. M. Mortland. 1974. Copper (II) interactions with montmorillonites: Evidence from physical methods. *Soil Sci. Soc. Amer. Proc.* **38**: 408–414.

Meads, R. E., and P. J. Malden. 1975. Electron Spin Resonance in natural kaolinites containing Fe³⁺ and other transition metal ions. *Clay Miner.* **10**: 313–345.

Mestdagh, M. M., A. J. Herbillon, L. Rodrique, and P. G. Rouxhet. 1982. Evaluation du rôle du fer structural sur la cristallinité des kaolinites. *Bull. Minéral.* **105**: 457–466.

Miyawaki, R., S. Tomura, S. Samejima, M. Okazaki, H. Mizuta, S. I. Maruyama, and Y. Shibasaki. 1991. Effects of solution chemistry on the hydrothermal synthesis of kaolinite. *Clays Clay Miner.* **39**: 498–508.

Mosser, C., M. Mestdagh, A. Decarreau, and A. Herbillon. 1990. Spectroscopic (ESR, EXAFS) evidence of Cu for (Al-Mg) substitution in octahedral sheets of smectites. *Clay Miner.* **25**: 271–282.

Mosser, C., A. Mosser, M. Romeo, S. Petit, and A. Decarreau. 1992. Natural and synthetic copper phyllosilicates studied by XPS. *Clays Clay Miner.* **40**: 593–599.

Mosser, C., S. Petit, and M. Mestdagh. 1993. ESR and IR evidences of chromium in kaolinites. *Clay Miner.* **28**: 353–364.

Pafomov, N. N., Yu. I. Tarasevich, E. G. Sivalov, and V. L. Sil'chenko. 1979. EPR and optical spectroscopic study of the state of copper (2+) exchange cations in montmorillonite and kaolinite. Dopov. Akad. Nauk. Ukr. SSSR, Ser. B: Geol., Khim. Biol. Nauki, (8), 642–646.

Paquet, H., J. Duplay, and D. Nahor. 1982. *Variations in the composition of phyllosilicates monoparticles in a weathering profile of ultrabasic rocks.* Developments in Sedimentology, 35, H. Van Olphen & F. Veniale Ed., Int. Clay Conf., Elsevier, 395–603.

Petit, S. 1990. Etude cristallochimique de kaolinites ferrifères et cuprifères de synthèse (150–250°C). Thesis, Poitiers. 237 pp.

Petit, S., and A. Decarreau. 1990. Hydrothermal (200°C) synthesis and crystal chemistry of iron-rich kaolinites. *Clay Miner.* **25**: 181–196.

Petit, S., T. Prot, A. Decarreau, C. Mosser, and M. C. Toledo-Groke. 1992. Crystallochemical study of a population of particles in smectites from a lateritic weathering profile. *Clays Clay Miner.* **40**: 436–445.

Pilipenko, A. T., B. Yu. Kornilovich, N. G. Vasil'ev, and V. I. Lysenko. 1987. Aqueous complexes of copper (II) on lateral faces of kaolinites and their transformation during mechanical activation. Dokl. Akad. Nauk. Ukr. SSSR, Ser. B: Geol., Khim. Biol. Nauki, (1), 52–54.

Pilipenko, A. T., B. Yu. Kornilovich, V. I. Lysenko, and V. V. Malyarenko. 1989. Aqueous complexes of copper (II) on the surface of activated kaolinites. Dokl. Akad. Nauk. Ukr. SSSR, (Phys. Chem) 305 (6), 1408–1411.

Plançon, A., and C. Tchoubar. 1977. Determination of structural defects in phyllosilicates by X-ray powder diffraction. II. Nature and proportion of defects in natural kaolinites. *Clays Clay Miner.* **25**: 436–450.

Plançon, A., R. F. Giese, and R. Snyder. 1988. The Hinckley index for kaolinites. *Clay Miner.* **37**: 203–210.

Plançon, A., R. F. Giese, R. Snyder, V. A. Drits, and A. S. Bookin. 1989. Stacking faults in kaolin-group minerals: Defect structures of kaolinite. *Clays Clay Miner.* **23**: 249–260.

Rengasamy, P. 1976. Substitution of iron and titanium in kaolinites. *Clays Clay Miner.* **24**: 264–266.

Shingh, B., and R. J. Gilkes. 1991. Weathering of a chromian muscovite to kaolinite. *Clays Clay Miner.* **39**: 571–579.

Sil'chenko, V. A., N. N. Pafomov, Yu. I. Tarasevich, I. V. Matyash, and Z. E. Suyunova. 1971. Electron paramag-

netic resonance of Cu^{2+} exchange cations in kaolinite. *Ukr. Khim. Zh., 37, (12),* 1238–1241.

Stubican, V., and R. Roy. 1961. Isomorphous substitution and infra-red spectra of the layer lattice silicates. *Amer. Miner.* **46**: 32–51.

Sun, M. S. 1963. The nature of chrysocolla from Inspiration mine, Arizona. *Amer. Miner.* **48**: 469–658.

Tomura, S., Y. Shibasaki, and H. Mizuta. 1983. Spherical kaolinite: Synthesis and mineralogical properties. *Clays Clay Miner.* **31**: 431–421.

Tomura, S., Y. Shibasaki, H. Mizuta, and I. Sunagawa. 1985a. Origin of the morphology of spherical kaolinite. *Clay Science* **6**: 159–166.

Tomura, S., Y. Shibasaki, H. Mizuta, and M. Kitamura. 1985b. Growth conditions and genesis of spherical and platy kaolinite. *Clays Clay Miner.* **33**: 200–206.

Van Oosterwyck-Gastuche, M. C. 1970. La structure de la chrysocolle. *C. R. Acad. Sc. Paris,* 271, p. 1837–1840.

Van Oosterwyck-Gastuche, M. C., and A. La Iglesia. 1978. Kaolinite synthesis. II. A review and discussion of the factors influencing the rate process. *Clays Clay Miner.* **26**: 409–417.

Weaver, C. E. 1976. The nature of TiO_2 in kaolinite. *Clays Clay Miner.* **24**: 215–218.

Wertz, J. E., and J. R. Bolton. 1972. *Electron Spin Resonance.* New York: Mc Graw-Hill.

Wilkins, R. W. T., and J. Ito. 1967. Infrared spectra of some synthetic talcs. *Amer. Miner.* **52**: 1649–1661.

Wolff, A. 1967. Contribution à l'étude des mécanismes de formation des argiles: Réaction de la silice en solution avec les cations Al^{3+}, In^{3+}, Ni^{2+} et Cu^{2+}. Thesis, Strasbourg, France, 85 p.